Study of Transfection Efficiencies of Cationic Glyconanoparticles of Different Sizes in Human Cell Line

Marya Ahmed,[†] Zhicheng Deng,[†,‡] and Ravin Narain*,[†,‡]

Department of Chemistry and Biochemistry, Laurentian University, 935 Ramsey Lake Road, Sudbury, Ontario P3E 2C6, Canada, and Department of Chemicals and Materials Engineering, University of Alberta, ECERF, Edmonton, Alberta T6G 2G6, Canada

ABSTRACT The growing attention toward the synthesis and uses of gold nanoparticles for biomedical applications is based on their biocompatibility, ease of functionalization, and unique optical and electronic properties. Recently, the gold nanoparticles are also found to induce the size-dependent interactions with living tissues. It has been found that gold nanoparticles of different sizes are uptaken by the cells in vitro and by the organs of living specimens in vivo at different rates. Herein, we report the use of gold nanoparticles of different sizes as a gene delivery agent. The gold nanoparticles of 10, 40, and 100 nm diameter were surface functionalized with cationic glycopolymer, and their biocompatibility under physiological conditions was investigated. The stable nanoparticles were then complexed with enhanced cyanine fluorescence protein plasmid (pECFP) and their transfection efficiencies in Hela cell line were studied. It was found that gold nanoparticles of 40 nm core diameter exhibit highest transfection efficiencies compared to the other sizes of nanoparticles studied.

KEYWORDS: cationic glycopolymer • citrate stabilized gold nanoparticles • surface functionalization • photochemistry • cytotoxicity • transfection efficiency

INTRODUCTION

The in vitro uses of gold nanoparticles for biomedical applications have already been established because of their unique optical and electronic properties, biocompatibility, and facile surface functionalization with the molecules of choice (1, 2). The extensive research on the morphology of gold nanoparticles has revealed interesting size- and shape-dependent functions of these metallic nanoparticles, which upon consideration can lead to the formation of biomaterials with improved properties (1−7). However, only a handful of reports discuss the size-dependent properties of gold nanoparticles, for biomedical purposes (4−8). Medley et al. focused upon the facile synthesis of colorimetric assay for the detection of cancerous cells, based upon the optical properties of gold nanoparticles (4). The use of fabricated gold nanoparticles in colorimetric assay for the cancer cells detection revealed that compared to the other sizes of gold nanoparticles, a significant shift in the surface plasmon band of gold nanoparticles was observed when gold nanoparticles of 20 nm in diameter were used (4). Schofield et al. also utilized the 16 nm gold nanoparticles to successfully synthesize the biosensor for cholera toxin detection (5).

The cellular uptake studies based on the comparison of rod-shaped gold nanoparticles with spherical nanoparticles show the preferential uptake of spherical nanoparticles by mammalian cells (6). Further studies revealed that the optimum diameter of nanoparticles required to stimulate the receptor mediated endocytosis of nanoparticles by human cells is 50 nm (6). The gold nanoparticles of this specific size are found to show the highest uptake by Hela cells because of their ability to undergo receptor-mediated endocytosis, when compared to the nanoparticles of other sizes (6, 7). Jin et al. extended the size-dependent study of metallic nanoparticles on semiconductor nanomaterials like carbon nanotubes and revealed that this size-dependent uptake of nanomaterials holds true for the nanoparticles other than gold nanoparticles as the carbon nanotubes exhibited the same size-dependent uptake around the diameter of 50 nm (9).

One of the well-studied applications of nanomaterials in vitro is their use as gene delivery agent (10−15). Gene therapy is one of the growing and extensively explored fields of biotechnology (16, 17). The fabrication of nanomaterials with cationic polymers and lipids provide the facile functionalization of nanoparticles with DNA, compared to the other covalent approaches used to anchor the DNA on the surface of nanoparticles (15, 18, 19). The binding of anionic DNA on the surface of nanoparticles by electrostatic interactions is preferred to obtain the optimum release of DNA from nanoparticles surface, as the strong attachment of nanoparticles with DNA can hinder the transcription process itself (15). A variety of cationic gold nanoparticles have been synthesized and their in vitro transfection efficiencies have been shown (10−15). The process of gene transfer by gold nanoparticles is typically facilitated by external impulse and

the transfection efficiencies are compared to either DNA alone or other commercially available agents (10−15). To the best of our knowledge, transfection efficiencies of gold nanoparticles of different core diameters, in the presence or absence of external impulse, has not yet been explored.

Herein, we report transfection efficiencies of gold nanoparticles of different core sizes. For this purpose, the cationic glycopolymer p(APMA$_{31}$-b-LAEMA$_{32}$) was synthesized by reversible addition−fragmentation chain transfer (RAFT) method, utilizing monomers 3-aminopropyl methacrylamide hydrochloride (APMA) and 2-lactobionamidoethyl methacrylamide (LAEMA). The gold nanoparticles were then surface functionalized with the cationic glycopolymer synthesized. The synthesis of cationic glycopolymer-stabilized gold nanoparticles of 10 nm in diameter and their transfection efficiencies have been previously reported in our group (20). To study the transfection efficiencies, gold nanoparticles of core diameter 10, 40, and 100 nm were surface functionalized with cationic glycopolymer p(APMA$_{31}$-b-LAEMA$_{32}$). The nanoparticles were first subjected to serum assay to confirm their stability in physiological conditions before assessing their implications in biological applications. The cationic glyconanoparticles were found to be stable in physiological conditions and subsequently complexed with pECFP-plasmid and the process was studied using agarose gel electrophoresis shift assay. The resulting complexes of plasmid−DNA and cationic glyconanoparticles formed at varying concentration of nanoparticles were used to transfect Hela cell line, and remarkable differences in transfection ability was noted, when glyconanoparticles of 10 nm core diameter were compared to those of 40 nm core diameter. The toxicity assay was also performed to determine the deleterious effects of cationic nanoparticles of different sizes in vitro after their use as gene delivery agent.

MATERIALS AND METHODS

Materials. All the chemicals and cell culture products were purchased from Sigma-Aldrich and were used without purification. The citrate stabilized gold nanoparticles were purchased from Ted Pella Inc.

Methods. *Polymer Characterization.* ^{1}H NMR spectra of the monomers and polymers were recorded on a Varian 200 MHz instrument.

Molecular weight and molecular weight distributions were determined by conventional Viscotek gel permeation chromatography (GPC) system using aqueous eluents, two Waters WAT011545 columns at room temperature and a flow rate of 1.0 mL/min using a 0.5 M sodium acetate/0.5 M acetic acid buffer as eluent. P(APMA) was characterized based on six near-monodisperse PEO standards (M_p = 1010−101200 g mol^{-1}). P(APMA-b-LAEMA) was characterized based on seven near-monodisperse Pullulan standards (M_w = 5900− 404000 g mol^{-1}).

Dynamic Light Scattering (DLS). Dynamic light scattering measurements were performed at room temperature using a Viscotek DLS instrument having He−Ne laser at a wavelength of 632 nm and pelltier temperature controller. p(APMA-b-LAEMA)-stabilized gold nanoparticles solutions were filtered through Millipore membranes (0.45 μm pore size). The data was recorded with OmniSize Software.

UV−Visible Spectroscopy. UV−visible absorption spectra (400- 800 nm) was recorded on a Cary UV 100 spectrophotometer from the aqueous solutions of p(APMA-b-LAEMA)-f-nanoparticles at room temperature.

Fluorescence Microscopy. Fluorescence microscopy was performed to detect the presence of CFP (enhanced cyanine fluorescence protein), by exciting the samples at λ = 433 nm and by collecting the emission spectrum at λ = 490 nm.

Plasmid Preparation and Purification. PECFP-N1, enhanced cyan fluorescent plasmid driven by cytomegalovirus (CMV) promoter, was transformed in super competent *E. coli* cells and amplified in 30 μg/mL Kanmycin containing LB broth media at 37 °C overnight with 225 rpm. After sufficient bacterial growth, the cells were pelleted by centrifugation at 2000g and 20 °C for 5 min followed by plasmid extraction using QIAGEN mini plasmid purification kit as per vendor's protocol. Plasmid purity was assessed by UV spectrophotometry ($A_{260/280}$ > 1.75), and agarose gel electrophoresis.

RAFT Diblock Copolymerization of 3-Aminopropyl Methacrylamide Hydrochloride (APMA) with 2-Lactobionamidoethyl Methacrylamide (LAEMA). APMA was first polymerized with CTP according to the previous report. Subsequently, p(APMA) (M_n = 5500 g/mol; M_w/M_n = 1.09) was used as macro chain transfer agent to synthesize p(APMA$_{31}$-b-LAEMA$_{32}$) diblock copolymer. As the second monomer, LAEMA (1.6 g) was added to p(APMA) solution (0.48 g in 8.0 mL of double distilled water) followed by the addition of 0.5 mL of ACVA (9.0 mg) *N,N*-Dimethylformamide (DMF) stock solution. After degassing via four freeze−thaw cycles, the flask was placed in a preheated oil bath for 15 h at 80 °C. The diblock copolymer p(APMA$_{31}$-b-LAEMA$_{32}$) was precipitated in acetone followed by washing with DMF.

Synthesis of Block Copolymer Coated 10 nm Sized Au Nanoparticles in the Presence of Irgacure-2959 (IRGC). The synthesis of 10 nm polymer-stabilized gold nanoparticles was carried out as described before. P(APMA$_{31}$-b-LAEMA$_{32}$) coated gold nanoparticles were synthesized by photoirradiation using Irgacure-2959 (IRGC) as a photo initiator. The molar ratio of HAuCl$_4$, IRGC, and p(APMA$_{31}$-b-LAEMA$_{32}$) in deionized water was 1:3:0.01. In a typical synthesis, the required amount of p(APMA$_{31}$-b-LAEMA$_{32}$) was dissolved in deionized water and the solution was added to HAuCl$_4$ (0.50 mg/mL) solution in deionized water. The mixture was stirred using a magnetic stirrer at room temperature for 20 min. Irgacure-2959 (15.3 mM, 1 mL) was dissolved in the mixture of deionized water and MeOH (4: 1, v/v). The Initiator solution was then added to the HAuCl$_4$ and p(APMA$_{31}$-b-LAEMA$_{32}$) mixture and stirred for 20 min. The photoirradiation of the reaction mixture was carried out using sixteen, 75 W UV lamps at wavelength of 300 nm in a Rayonet photo reactor (Southern N.E. Ultraviolet Co.) After 5 min, the reaction mixture was taken off the photo reactor and stirred at room temperature. The gold nanoparticles produced were centrifuged at 20000 rpm for 2 h to remove the excess polymer. The pellet was resuspended in deionized water.

Surface Functionalization of 40 and 100 nm Citrate-Stabilized Gold Nanoparticles by Cationic Glycopolymer p(APMA$_{31}$-b-LAEMA$_{32}$). P(APMA$_{31}$-b-LAEMA$_{32}$) stabilized gold nanoparticles were prepared by mixing commercial gold nanoparticles with cationic glycopolymer solution with some modifications to the previously reported procedure (27). Briefly, 500 μL of commercially available gold nanoparticles of 40 nm and 100 nm were added to 1 and 2.5 μM glycopolymer solutions, respectively at pH 7.4. The reaction was allowed to occur at room temperature for 3 h and nanoparticles produced were stored at 4 °C overnight. The purification of polymer stabilized gold nanoparticles was obtained by centrifuging the reaction solution at 20 000 rpm for 2 h and resuspending the nanoparticles in deionized water. The surface functionalization of gold nanoparticles by glycopolymer before and after the centrifugation was studied using dynamic light scattering and UV−visible spectroscopy.

Serum Assay. The cationic polymer stabilized gold nanoparticle of sizes 10, 40, and 100 nm were centrifuged at 20 000 rpm for two hours and the pellet was suspended in deionized water, phosphate buffer saline, and 10% v/v human serum, separately. Then the change in size of gold nanoparticles was measured by UV–vis measurement in the wavelength range of 400–700 nm.

DNA Complexation. DNA complexation of gold nanoparticles was studied using agarose gel electrophoresis. The varying concentrations of different sizes of gold nanoparticles were complexed with 350 ng of pECFP-N1 plasmid and the complexes were loaded into 0.7% agarose gel. The gel was electrophoresed for one hour at 70 V, and the complexes were characterized after staining the gel with 0.5 μg/mL of ethidium bromide. The images were obtained on an ultraviolet transilluminator.

Transfection. Hela cells were maintained in Dulbecco's modified Eagles' medium, supplemented with 10% fetal bovine serum at 37 °C, in a humidified 5% CO_2 atmosphere, as described above. Before the experiment, 2000 Hela cells were seeded in a 96-well tissue culture plate and were allowed to adhere overnight. The test samples were prepared for each well by mixing 0.35 μg of pECFP-plasmid with varying amounts of cationic gold nanoparticles of 10 and 40 nm, separately. The mixture was incubated for 15 min and was added to the cells, the plate was incubated for 6 h at 37 °C, in serum free medium. The cells were washed three times with Dulbecco's phosphate buffer (DPBS) and were allowed to grow for another 48 h in fresh culture medium supplemented with 10% FBS. The gene expression was evaluated using fluorescent microscopy. The presence of CFP protein was confirmed using the emission spectrum of cyanine fluorescence protein at 490 nm.

Toxicity Assays. *Toxicity Assay for Glycopolymer.* **1.** *Preparation of Polymer Stock Solutions.* All polymers were dissolved into Dulbecco's phosphate buffer at a final concentration of 0.6 mM. The samples were autoclaved and different volumes of prepared solution were added into different volumes of DMEM medium to obtain the final concentration of 0.5, 1, and 2 μM of polymer in the medium.

2. *Cytotoxicity Test.* Cytotoxicity was characterized using MTT assay. Hela cells were plated in 96-well plate at the density of 10000 cells/well in 100 μL of serum and antibiotic supplemented growth medium. Cells were incubated for 24 h at 37 °C and 5% CO_2, after which the growth medium was replaced with DMEM medium containing different concentrations of polymers, prepared above p(APMA$_{31}$-*b*-LAEMA$_{32}$). The cells were further incubated for 24 h under the same conditions, after which 25 μL of MTT dye was added to each well and plate was incubated for 2 h. Next, 100 μL of MTT lysis solution was added to each well and cells were incubated overnight. Absorbance was measured at 570 nm with power wave instrument. Survival percentage was calculated by comparison to untreated cells (100% survival).

Toxicity Assay on Transfected Cells. Hela cells maintained at 80% confluency were seeded at 2000 cells/well in a 96-well plate and were allowed to adhere overnight. The varying concentrations of 10 and 40 nm gold nanoparticle-plasmid complexes in serum-free medium were added to each well and each experiment was done in triplicate. After 6 h, the medium was changed to serum-containing medium and cells were allowed to grow for another 48 h. The cell viability was tested using the MTT assay as described above.

RESULTS AND DISCUSSION

Gold nanoparticles are one of the well-explored topics of nanotechnology, in terms of their size-dependent optical, electronic, and biological properties (1, 2). The study of these unique properties of gold nanoparticles emphasized toward

Scheme 1. Transfection Efficiencies of p (LAEMA$_{32}$-*b*-APMA$_{31}$)-*f*-gold Nanoparticles of 40 nm Core Diameter
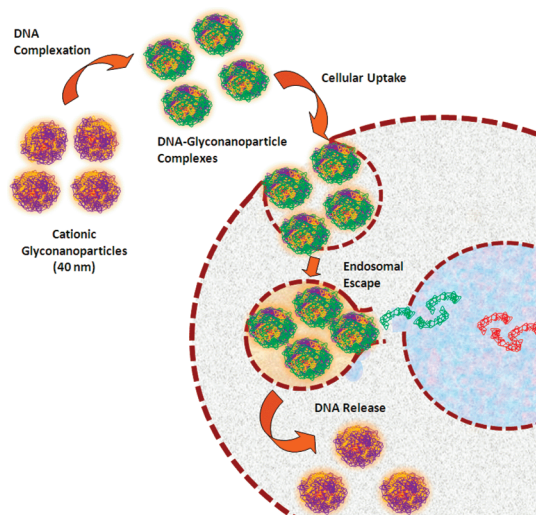
the development of facile methods for the synthesis of size-controlled monodisperse gold nanoparticles that can be further utilized for a variety of purposes (21). These size-dependent properties of nanoparticles are also found to impact their uses for biological and biomedical applications (6–9). Gene delivery methods have extensively been studied in an effort to overcome the physiological barriers confronted during the gene transfer (16). The cationic moieties functionalized gold nanoparticles have also been utilized for this purpose and are shown to produce enhanced gene transfer by reducing some of the intracellular barriers during the gene delivery process (9–14, 20).

Chithrani et al. have studied the uptake and release of different sizes of gold nanoparticles into and out of Hela cells (6). The process was further studied in detail to determine the size-dependent uptake of different sizes of gold nanoparticles, surface functionalized by the biomolecules. However, no change in uptake mechanism of nanoparticles was observed indicating that it was not the surface chemistry, but the dimensions of nanoparticles, responsible for the pronounced effect observed during in vitro studies (7). The results indicated that spherical gold nanoparticles of around 50 nm are interesting because of their ability to undergo receptor mediated endocytosis, higher cellular uptake, and single entry into the cell, compared to the other sizes of nanoparticles (7). These properties observed for the gold nanoparticles of the specific dimensions make them ideal for gene therapy purposes, as the potential of improving the gene delivery vehicle relies on its monodispersity, ability to undergo receptor mediated endocytosis, and higher cellular uptake, regardless of the charge on the surface of vehicle (16). To assess these characteristics of nanoparticles for gene delivery applications, we propose transfection efficiencies of gold nanoparticles of different sizes in the Hela cell line. The gold nanoparticles utilized for this purpose possess core diameter of 10, 40, and 100 nm. Gold nanoparticles of these sizes were surface-functionalized with cationic glycopolymer

in an effort to synthesize an ideal gene delivery vehicle with reduced toxicity.

The cationic glycopolymer of molar mass 20 kDa was prepared by reversible addition—fragmentation chain transfer (RAFT) method, and was characterized with ^{1}H NMR and GPC techniques (see the Supporting Information, Figure S1 and S2 and Table S1). The detailed synthesis and characterization of glycopolymer and its cationic block copolymer has been reported (22, 23). The applications of nanomaterials for biological purposes are largely dependent upon the types of methods used for their synthesis. RAFT is one of the recently developed polymerization techniques to produce monodisperse polymers for biomedical purposes (24). The synthesis and in vitro uses of glycopolymers for biomedical applications is relatively new but rapidly growing aspect of nanotechnology (25). Recently, glyconanoparticles are envisaged for various biomedical applications because of the biocompatibility of the glycopolymers and their tendency to enhance cellular interactions with the glycopolymer segment of the vehicle because of the "cluster glycoside effect" (25, 26). The toxicity of the cationic glycopolymer with its corresponding neutral glycopolymer was tested and compared by MTT assay using Hela cell line. It was found that there was no significant difference in the toxicity of cationic glycopolymer, compared to its corresponding homo glycopolymer, indicating that glycopolymer segment of the block copolymer can successfully mask the cationic component of the polymer, thus reducing the toxicity of the cationic vehicle during in vitro studies (see the Supporting Information, Figure S3).

The citrate-stabilized gold nanoparticles of 40 and 100 nm were surface functionalized with p (APMA$_{31}$-b-LAEMA$_{32}$) to facilitate their complexation with anionic plasmid—DNA. Miyamoto et al. has reported the surface functionalization and characterization of the citrate stabilized gold nanoparticles of diameter ~18.4 nm with cationic block copolymer PEG-b-PAMA (27). However, the synthesis of the polymer was obtained by atom transfer radical polymerization (ATRP), limiting their use in biological applications, because of the possible presence of residual metal catalyst (23). The biological applications for these cationic block copolymer-modified nanoparticles were also not investigated. We report the surface modification of citrate-stabilized gold nanoparticles of different sizes (40 and 100 nm) by cationic glycopolymer via a slight modification to the previously reported method (26). The surface area of nanoparticles largely dictates their interactions with living systems. It has been found that the surface area of cationic nanoparticles strongly correlate with their ability to disrupt the lipid bilayer. The surface area of nanoparticles, when defined in term of mass of a sample, indicates that smaller nanoparticles possess greater surface area and vice versa (28). However, here we are dealing with the number of particles in the given sample. Leroueil et al. has defined the surface area of nanoparticles in terms of number of particles and it states that for a given number of nanoparticles, the larger particles possess greater surface area, hence showing greater disruption ability of lipid bilayer
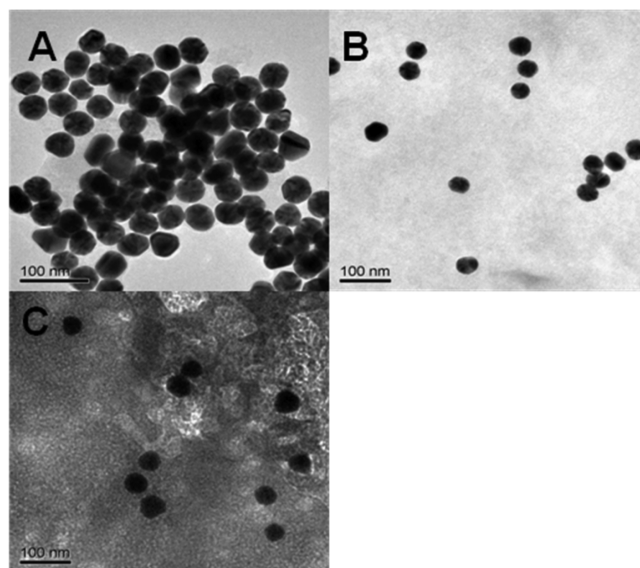

FIGURE 1. TEM images of 40 nm gold nanoparticles: (A) citrate-stabilized gold nanoparticles, (B) p(APMA-b-LAEMA)-functionalized gold nanoparticles, (C) plasmid-functionalized glycopolymer-stabilized gold nanoparticles.

(29). Thus, as expected, the particles with greater surface area (100 nm) would require a higher concentration of glycopolymers to completely cover the surface of nanoparticles compared to the particles with smaller surface area (40 nm). The further increase in concentration of cationic glycopolymer led to the aggregation and precipitation of nanoparticles from solution. This was measured by the decrease in intensity and broadening of surface plasmon band of UV—vis spectrum, indicating the optimum concentrations required for the functionalization of nanoparticles. The cationic glyconanoparticles thus produced were stable for weeks and did not show any aggregation.

The capping of citrate-stabilized gold nanoparticles of 40 and 100 nm diameter with cationic glycopolymers was studied by UV—visible spectroscopy. The UV—vis spectra showed a slight red shift after the attachment of cationic glycopolymer on the surface of gold nanoparticles. (see Figures 2 and 3 and the Supporting Information, Figures S4 and S5) The exact mechanism of stabilization of anionic nanoparticles with cationic polymers is unclear (27). Miyamoto et al. suggested that formation of Au—N (16.7 kJ) bond between gold and amine moiety of polymer is more likely as compared to the electrostatic interactions to explain the stabilization of nanoparticles by cationic polymers (27). Our results further support this hypothesis, as mere electrostatic interactions between the polymer and gold nanoparticles cannot be strong enough to facilitate their use as gene delivery vehicle and impart their stability under physiological conditions.

The capping process of 40 nm gold nanoparticles was further studied by TEM and no aggregation of particles was observed after their surface functionalization with cationic glycopolymer (Figure 1). It should be noted that lower concentrations of surface-functionalized gold nanoparticles in Figure 1B as compared to citrate-capped nanoparticles shown in Figure 1A is due to the higher dilutions of nano-
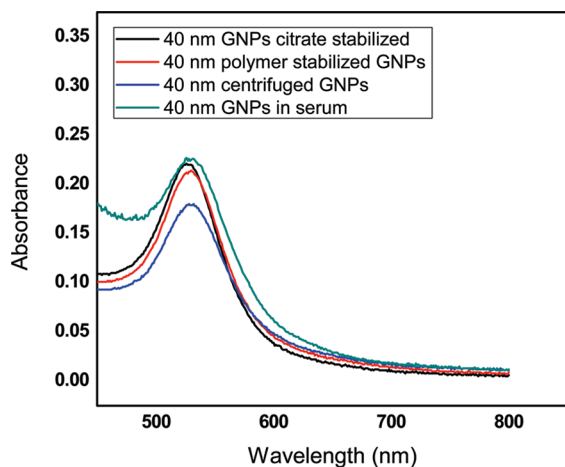
FIGURE 2. Stepwise study of UV–vis spectra of gold nanoparticles of 40 nm in diameter, before and after their surface functionalization with p(LAEMA-*b*-APMA), before and after their purification, and after their dispersion in 10% FBS.
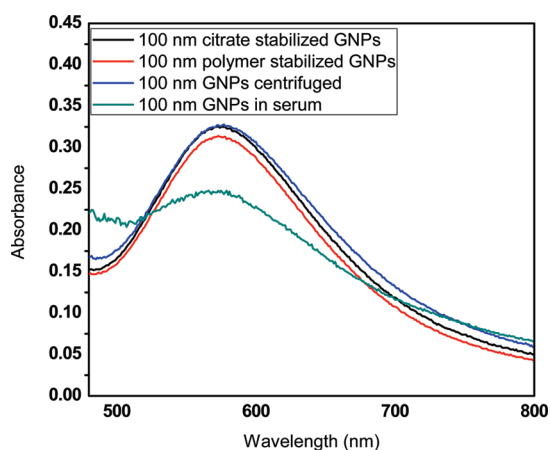

FIGURE 3. Stepwise study of UV–vis spectra of gold nanoparticles of 100 nm in diameter, before and after their surface functionalization with p (LAEMA-*b*-APMA), before and after their purification, and after their dispersion in 10% FBS.

particles required during the functionalization process. The use of higher concentration of nanoparticles during surface functionalization led to the rapid precipitation of particles from the solution.

Cationic glycopolymer stabilized gold nanoparticles were synthesized in one step via a photochemical process (30). The synthesis of near monodisperse cationic glyconanoparticles of 10 nm in diameter has been well studied (20). The cationic nanoparticles thus produced were found to be biocompatible and were able to mediate gene transfer in the absence of external stimulus during in vitro studies (20). The p(APMA$_{31}$-*b*-LAEMA$_{32}$)-*f*-gold nanoparticles were produced in one step using Irgacure 2959 as photoinitiator. The production of ketyl radicals upon exposure to UV radiation initiated the synthesis of monodisperse gold nanoparticles, while the presence of cationic polymer in the solution subsequently capped the nanoparticles during the procedure, thus facilitating the synthesis of monodisperse nanoparticles, as described by previous methods of synthesis (30). The p(APMA$_{31}$-*b*-LAEMA$_{32}$)-*f*-gold nanoparticles were produced under same conditions used earlier for the synthesis of p(APMA$_{38}$-*b*-GAPMA$_{45}$)-*f*-gold nanoparticles, and
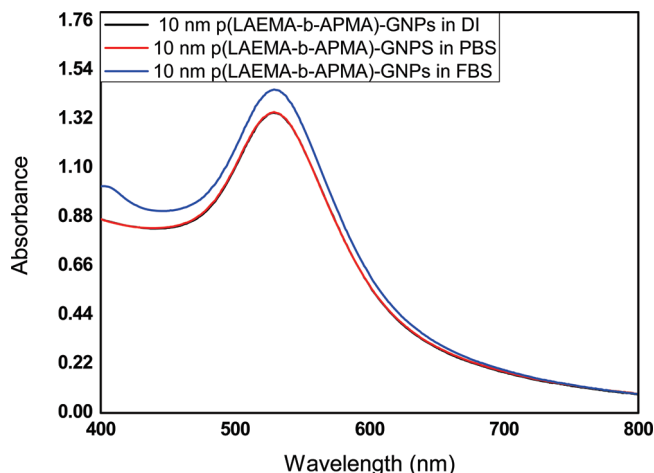

FIGURE 4. UV–vis spectra of gold nanoparticles of 10 nm in diameter before and after their dispersion in high salt solution and in 10% v/v fetal bovine serum.

thus gold nanoparticles produced were identical in size and differ only by the presence of different carbohydrate moieties on the surface of nanoparticles (20).

The biocompatibility of cationic polymer modified gold nanoparticles of different sizes was assessed by the dispersion of nanoparticles in high salt and serum conditions. The citrate stabilized gold nanoparticles are reported to be non toxic but suffer from aggregation, when subjected to physiological conditions (2). The immediate aggregation of citrate stabilized gold nanoparticles upon exposure to high salt solution was also observed by our group and UV–vis spectra could not be obtained after the exposure due to their rapid precipitation from solution (see Figure 4). The p(APMA$_{31}$-*b*-LAEMA$_{32}$)-*f*-gold nanoparticles were then subjected to serum assay to determine the stability of nanoparticles of different sizes in physiological conditions.

The figures indicated that smaller nanoparticles (10 and 40 nm) were reasonably stable in physiological conditions, as no shift of the UV–vis peak was observed before and after their suspension in 10% serum solution, even after overnight incubation in these conditions. However, for the larger nanoparticles (100 nm), rapid precipitation was noted within minutes of their dispersion in physiological media, rendering them unsuitable for the biological uses.

The functionalization of cationic gold nanoparticles with anionic plasmid–DNA by electrostatic interactions was studied using agarose gel electrophoresis shift assay to determine the concentration of nanoparticles required to obtain the complete complexation of plasmid–DNA (see the Supporting Information, Figures S6 and S7). The number of cationic gold nanoparticles of 10 nm core diameter in the given volume of solution was calculated using the formula

$$N_{Au} = 4\pi(d/2)^3/V_{Au}$$

Where N_{Au} is mean number of gold atoms in one sphere and *d* is diameter of the particles (2). The number of nanoparticles of 10 nm core diameter in given volume were then calculated by obtaining the total number of gold atoms in

the solution and then dividing the mean number of gold atoms in one sphere by total number of gold atoms in the solution. The calculations showed that 380×10^9 nanoparticles of 10 nm core diameter could completely condense 350 ng of pECFP plasmid. The number of nanoparticles of 40 nm core diameter per milliliter of solution were provided by Ted Pella Inc., and further calculations were done according to the experimental procedure to estimate the average number of nanoparticles in the given volume of solution. The results showed that compared to smaller nanoparticles, where 380×10^9 particles were required to completely condense the given amount of plasmid, cationic nanoparticles of 40 nm core diameter required 18×10^9 particles to condense the same amount of plasmid. TEM images of 40 nm gold nanoparticles obtained after surface functionalization with plasmid further confirmed their monodispersity, after functionalization. The images obtained show that incubation of plasmid with the excess of nanoparticles maintains the monodispersity of nanoparticles and big aggregates of cationic nanoparticles around the anionic macromolecules, at the given concentration, have not been observed.

The gene delivery vehicles of two different sizes thus synthesized were used for transfection purposes in Hela cells. The size-dependent properties of gold nanoparticles have been explored in detail, and the experiments were performed using Hela cell line (6, 7). As different cells respond differently to the external material, we used the same cell line to explore the transfection efficiencies of cationic gold nanoparticles of two different sizes in an effort to prevent the cell selective response in the uptake and processing of these nanomaterials by a different cell line (6, 30). The transfection efficiencies of p(APMA$_{38}$-b-GAPMA$_{45}$)-f-gold nanoparticles in the Hela cell line are also studied in detail (20). As discussed earlier, p(APMA-b-LAEMA)-f-gold nanoparticles of 10 nm core diameter are identical to those of p(APMA$_{38}$-b-GAPMA$_{45}$)-f-gold nanoparticles, in terms of size and DNA condensation ability, the molecular weight of two polymers used for nanoparticles synthesis and their cationic characters are identical. However, the difference in carbohydrate segment of the two polymers does produce significant differences in biological characteristics of the gene delivery vehicles. It has been observed that p(APMA$_{38}$-b-GAPMA$_{45}$)-f-nanoparticles exhibited pronounced gene transfer ($\sim$45%) in the absence of external impulse; in contrast, p(APMA$_{31}$-b-LAEMA$_{32}$)-f-nanoparticles showed lower degree of gene transfer under the same conditions, and the gene transfer efficiency of 10 nm gold nanoparticles was found to be up to 25% only. Reineke et al. has recently studied the effect of glycopolymer segment on the transfection efficiencies of cationic glycopolymers, and it has been reported that stereochemistry of hydroxyl groups plays a dominant role in gene transfection ability. They also showed comparatively higher transfection efficiencies of glucose functionalized cationic nanoparticles compared to other cationic monosaccharides stabilized nanoparticles (25).
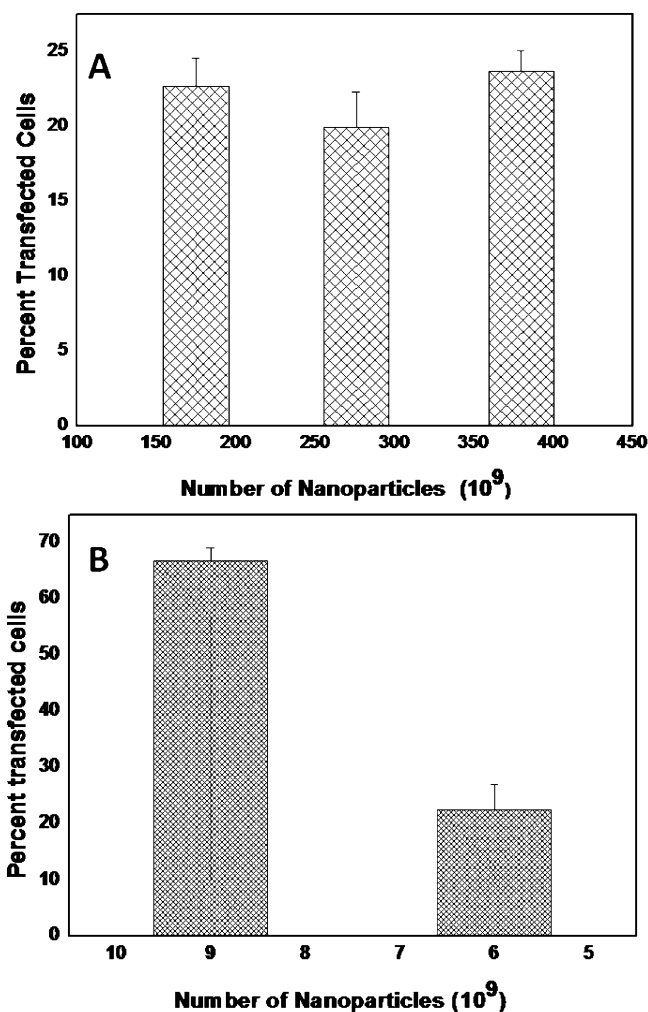

FIGURE 5. Gene transfection efficiencies of Hela cells upon treatment with cationic glyconanoparticle−plasmid complexes. (A) Transfection efficiencies of 10 nm gold nanoparticles in Hela cells upon their incubation with pECFP plasmid−nanoparticle complex at 37 °C. (B) Transfection efficiencies of 40 nm gold nanoparticles in Hela cells upon their incubation with pECFP plasmid−nanoparticle complex at 37 °C.

The transfection efficiencies of pECFP-plasmid-functionalized gold nanoparticles of core diameter 10 and 40 nm were then compared (see Figure 5). The transfection efficiencies were studied by detecting the presence of CFP protein in the transfected cells, using fluorescence microscopy. The transfected cells were excited at $\lambda_{ex} = 433$ nm and the emission spectrum was collected at $\lambda_{em} = 490$ nm. The glowing cells detected under the microscope confirmed the expression of CFP protein, which were then divided with total number of cells in the field of view, to obtain the percent cells transfected in the given treatment. Each experiment was performed in triplicate to calculate the random error between samples, and the experiments were repeated twice to confirm the reproducibility of the data The values of transfection efficiencies obtained were normalized compared to the untreated cells and plasmid alone and it was found that gold nanoparticles of 40 nm in diameter can transfect Hela cells with much greater efficiencies, in the absence of an external impulse, compared to the gold nanoparticles of core diameter 10 nm. The larger nanopar-

ticles exhibited the transfection efficiencies of ~65–70%, as compared to smaller particles, which showed much lower levels of gene transfection (~20–25%).

It should be noted that transfection experiments were performed with net negative charge on the plasmid–nanoparticle complex for larger particles, as determined by agarose gel electrophoresis, because of the toxicity limitation for these nanomaterials at higher concentrations. However, for the smaller nanoparticles, transfection studies were obtained at various ratios of net positive charge. As expected, the increase in number of nanoparticles of 40 nm core diameter increases the transfection efficiencies due to the increase in net cationic character of the vehicle (see Figure 5B). In contrast, plasmid–nanoparticle complexes of smaller nanoparticles (10 nm) possessed net cationic character, thus further increase in concentration of smaller nanoparticles did not significantly affect the transfection values. Although the cationic nanoparticle–plasmid complexes are known to transfect at higher levels than nanoparticle–plasmid complex with net anionic character, the results obtained show that gold nanoparticles of core diameter 40 nm with net negative charge on the plasmid–nanoparticle complex transfect at much higher levels than the others despite the presence of net positive charge on the latter (16). The ability of cationic nanoparticles to undergo receptor-mediated endocytosis is well-known. The cellular uptake of cationic delivery vehicle predominantly occurs through electrostatic interaction between cationic nanoparticle–DNA complexes and anionic cell surface proteoglycans, regardless of the specificity of the vehicle. The cationic vehicles then undergo "enforced" endocytosis because of the electrostatic interactions between the vehicle and the host cells, thus contributing toward the higher chances of successful gene transfer (16). It has also been shown that cationic glyconanoparticle–oligonucleotide complexes possessing a net cationic charge possess the ability to undergo receptor-mediated endocytosis (20). The uptake of ~50 nm gold by receptor mediated endocytosis, regardless of the surface charge of the nanoparticle–plasmid complex, is also well-studied (6, 7). Thus, it is thought that this difference in transfection efficiencies of nanoparticles of different sizes can best be explained by the difference in core diameter of two sizes of nanoparticles. The gold nanoparticles of larger size (~40 nm) maintain their monodispersity after their surface functionalization with plasmid and show higher uptake by Hela cells, which leads to the decreased electrostatic interactions between plasmid and nanoparticles thus contributing toward facile release of plasmid from the vehicles and higher gene expression. In contrast, gold nanoparticles of smaller size aggregate and completely complex the plasmid, which may lead to the slow release of plasmid from strong cationic component of the vehicles thus contributing toward lower gene transfection efficiency.

The toxicity of nanomaterials is an important factor for their use in transfection experiments. Although at high
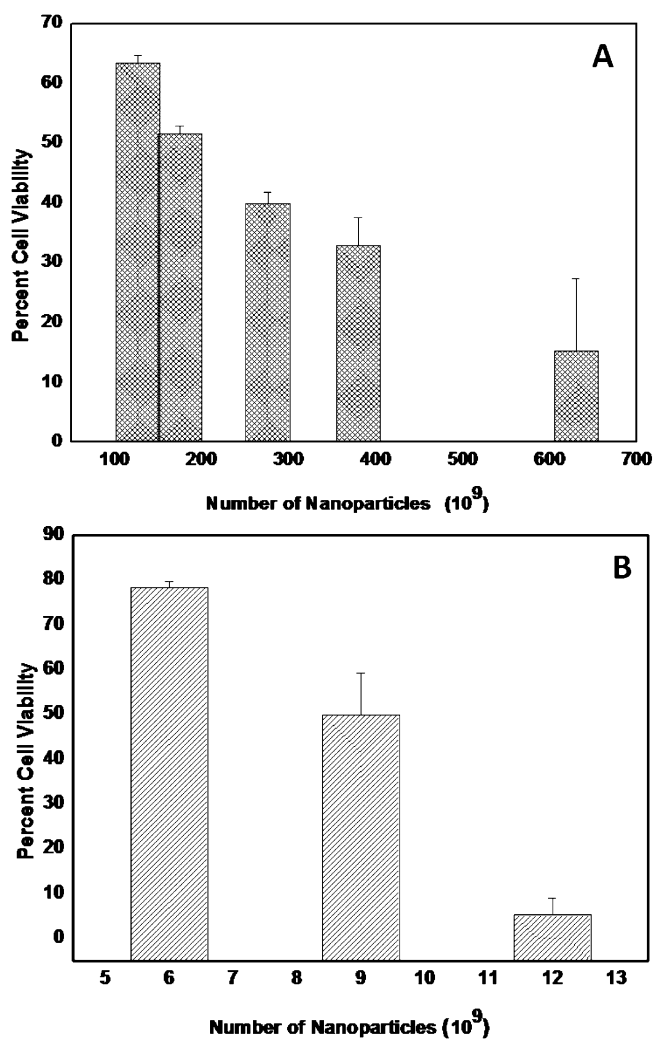

FIGURE 6. Cell viability values of Hela cells upon treatment with cationic glyconanoparticle–plasmid complexes. (A) Normalized viability of Hela cells transfected with 10 nm glyconanoparticles–plasmid complex, determined by MTT assay. (B) Normalized viability of Hela cells transfected with 40 nm glyconanoparticles–plasmid complex, determined by MTT assay.

enough concentration all nanoparticles are toxic, the term toxicity is more meaningful in the context of application of materials (31). The higher toxicity of cationic nanoparticles compared to their anionic counterparts is well-established because of the higher disruption ability of cationic nanoparticles, regardless of the size and shape (27, 31). In contrast to various studies, where anionic or biomolecule-stabilized gold nanoparticles are found to be inert, the cationic nanoparticles of same dimensions are reported to be significantly toxic (6, 7, 27, 31–33). Pan et al. has studied the cytotoxicity of gold nanoparticles in different cell lines including Hela cells and has reported that the cytotoxicity of nanomaterials is dependent on their capping ligand (34). The toxic effects of cationic nanomaterials of two different sizes after transfection are studied using the MTT assay of cell viability on Hela cells (Figure 6).

The concentration of cationic glycopolymer required to functionalize the surface of larger nanoparticles (40 nm) is 1.5 μM, and the MTT results show that at this concentration the glycopolymer segment can mask the cationic compo-

nent of the polymer (see the Supporting Information, Figure S3). The higher toxicity of larger particles is attributed to the higher disruption ability of the nanoparticles after the release of plasmid form the complex, as compared to the smaller particles, because of the larger cationic component of that vector. The results reported here are in agreement with the previous studies, which show the higher toxicity values for cationic nanoparticles containing larger surface area (29).

CONCLUSION

In short, the study of transfection efficiencies of gold nanoparticles of two different core diameters has been reported. It is found that the larger nanoparticles of 40 nm core diameter showed enhanced gene transfection, possibly because of their monodispersity, higher cellular uptake, and optimum electrostatic interactions between DNA and cationic polymer, thus maximizing the release of plasmid from the cationic vehicle. In contrast, smaller nanoparticles are able to undergo receptor-mediated endocytosis and showed lower gene transfer ability, probably because of the stronger interactions of nanoparticles with DNA preventing the optimum release of plasmid from the nanoparticle complex. The higher gene transfer of larger nanoparticles is also accompanied by higher toxicity of these nanoparticles. Further studies are required to investigate the exact mechanism of this behavior of nanoparticles and to find the bioconjugation techniques that can overcome the toxicity issues of larger nanoparticles for gene transfection purposes.

Supporting Information Available: GPC and ^{1}H NMR data of block copolymer synthesis, toxicity results of the polymers, UV−vis spectrum of gold nanoparticles showing their functionalization, agarose gel electrophoresis for the complexation of DNA to gold nanoparticles, and transfection images (PDF). This material is available free of charge via the Internet at http://pubs.acs.org.

REFERENCES AND NOTES

(1) Murray, C. B.; Kagan, R. C. *Annu. Rev. Mater. Sci.* **2000**, *30*, 545–610.
(2) Daniel, C.-M.; Astruc, D. *Chem. Rev.* **2004**, *104*, 293–346.
(3) Ghosh, K. S.; Pal, T. *Chem. rev.* **2007**, *107*, 4797–4862.
(4) Medley, D. C.; Smith, E. J.; Tang, Z.; Wu, Y.; Bamrungsap, S.; Tan, W. *Anal. Chem.* **2008**, *80*, 1067–1072.
(5) Schofield, L. C.; Field, A. R.; Russell, A. D. *Anal. Chem.* **2007**, *79*, 1356–1361.
(6) Chithrani, D. B.; Ghazani, A. A.; Chan, W. C. W. *Nano Lett.* **2006**, *6*, 662–668.
(7) Chithrani, D. B.; Chan, W. C. W. *Nano Lett.* **2007**, *7*, 1542–1550.
(8) De Job, H. W.; Hagens, I. W.; Krystek, P.; Burger, C. M.; Sips, J. A. M. A.; Geertsma, E. R. *Biomaterials.* **2007**, *12*, 1912–1919.
(9) Jin, H.; Heller, A. D.; Sharma, R.; Strano, S. M. *ACS Nano* **2009**, *3*, 149–158.
(10) Snadhu, K. K.; McIntosh, M. C.; Simard, M. J.; Smith, W. S.; Rotello, M. V. *Bioconjugate Chem.* **2002**, *13*, 3–6.
(11) Wang, H.; Chen, Y.; Li, X.-Y.; Liu, Y. *Mol. Pharm.* **2007**, *4*, 189–198.
(12) Ghosh, S. P.; Kim, C.-K.; Han, G.; Forbes, S. N.; Rotello, M. V. *ACS Nano* **2008**, *2*, 2213–2218.
(13) Liu, Y.; Franzen, S. *Bioconjugate Chem.* **2008**, *19*, 1009–1016.
(14) Zhou, X.; Zhang, X.; Yu, X.; Zha, X.; Fu, Q.; Liu, B.; Wang, X.; Chen, Y.; Chen, Y.; Shan, Y.; Jin, Y.; Wu, Y.; Liu, J.; Kong, W.; Shen, J. *Biomaterials.* **2008**, *29*, 111–117.
(15) Kawano, T.; Yamagata, M.; Takahashi, H.; Niidome, Y.; Yamada, S.; Katayama, Y.; Niidome, T. *J. Controlled Release* **2006**, *111*, 382–389.
(16) Mintzer, A. M.; Simanek, E. E. *Chem. Rev.* **2009**, *109*, 259–302.
(17) Pun, S. H.; Davis, E. M. *Bioconjugate Chem.* **2002**, *13*, 630–639.
(18) Narang, S. A.; Thoma, L.; Miller, D. D.; Mahato, I. R. *Bioconjugate Chem.* **2005**, *16*, 156–168.
(19) Nitin, N.; Javier, J. D.; Richards-Kortum, R. *Bioconjugate Chem.* **2007**, *18*, 2090–2096.
(20) Ahmed, M.; Deng, Z.; Liu, S.; Lafrenie, R.; Kumar, A.; Narain, R. *ACS Nano* **2009**, submitted.
(21) Dahl, A. J.; Maddux, S. L. B.; Hutchison, E. J. *Chem. Rev.* **2007**, *107*, 2228–2269.
(22) Deng, Z.; Ahmed, M.; Narain, R. *J. Polym. Sci., Part A* **2008**, *47*, 614–627.
(23) Deng, Z.; Bouchekif, H.; Babooram, K.; Housni, A.; Choytun, N.; Narain, R. *J. Polym. Sci., Part A* **2008**, *46*, 4984–4996.
(24) Lowe, B. A.; Wang, R. *Polymer* **2007**, *48*, 2221–2230.
(25) Liu, Y.; Reineke, T. M. *J. Am. Chem. Soc.* **2005**, *127*, 3004–3015.
(26) (a) De la Fuente, M. J.; Barrientos, G. A.; Rojas, C. T.; Rojo, J.; Canada, J.; Fernandez, A.; Penades, S. *Angew. Chem.* **2001**, *113*, 2318–2321. (b) Barrientos, G. A.; De la Fuente, M. J.; Rojas, C. T.; Fernandez, A.; Penades, S. *Chem.— Eur. J.* **2003**, *9*, 1909–1921. (c) Fuente, M. J.; Alcantara, D.; Penades, S. *IEEE Trans. Nanobiosci.* **2007**, *6*, 275–281.
(27) Miyamoto, D.; Oishi, M.; Kojima, K.; Yoshimoto, K.; Nagasaki, Y. *Langmuir* **2008**, *24*, 5010–5017.
(28) Oberdorster, G.; Oberdorster, E.; Oberdorster, J. *Environ. Health Perspect.* **2005**, *113*, 823–839.
(29) Leroueil, R. P.; Berry, A. S.; Duthie, K.; Han, G.; Rotello, M. V.; McNerry, Q. D.; Baker, R. J.; Orr, G. B.; Holl, B. M. M. *Nano Lett.* **2008**, *8*, 420–424.
(30) (a) Mcgilvray, L. K.; Decan, R. M.; Wang, D.; Scaiano, C. J. *J. Am. Chem. Soc.* **2006**, *128*, 15980–15981. (b) Narain, R.; Housni, A.; Gody, G.; Boullanger, P.; Charreyre, M.; Delair, T. *Langmuir* **2007**, *23*, 12835–12841. (c) Housni, A.; Ahmed, M.; Liu, S.; Narain, R. *J. Phys. Chem. C* **2008**, *112*, 12282–12290.
(31) Patra, K. H.; Banerjee, S.; Chaudhuri, U.; Lahiri, P.; Dasgupta, K. A. *Nanomed.: Nanotechnol., Biol., Med.* **2007**, *3*, 111–119.
(32) Murphy, J. C.; Gole, M. A.; Stone, W. J.; Sisco, N. P.; Alkilany, M. A.; Goldsmith, C. E.; Baxter, C. S. *Acc. Chem. Res.* **2008**, *41*, 1721–1730.
(33) Xu, C.; Tung, A. G.; Sun, S. *Chem. Mater.* **2008**, *20*, 4167–4169.
(34) Pan, Y.; Neuss, S.; Leifert, A.; Fischler, M.; Wen, F.; Simon, U.; Schmid, G.; Brandau, W.; Jahnen-Dechent, W. *Small* **2007**, *3*, 1941–9149.

AM900357X